

# **SOUND TRANSMISSION ACROSS FINITE CLAMPED DOUBLE-WALL SANDWICH PANELS IN THE PRESENCE OF EXTERNAL MEAN FLOW**

Jean-Cédric Catalan

*ENSTA ParisTech, Department of Mechanical Engineering, Palaiseau, France*

Yu Liu

*Southern University of Science and Technology, Department of Mechanics and Aerospace Engineering, Shenzhen, P. R. China*

*email: liuy@sustc.edu.cn*

This paper studies the effects of an external mean flow on the sound transmission through finite clamped double-wall sandwich panels lined with poroelastic materials. Biot's theory is employed to describe wave propagation in poroelastic materials. The clamped boundary of finite panels are dealt with by the modal superposition theory and the weighted residual (Garlekin) method, leading to a matrix equation solution for the sound transmission loss (STL) through the structure. The theoretical model is validated against existing theories of infinite sandwich panels with and without an external mean flow. It is shown that the external flow has significant effects on the STL which are coupled with the clamped boundary effect dominating in the low-frequency range.

**Keywords:** sandwich panels, external mean flow, poroelastic material, clamped boundary

---

## **1. Introduction**

Double-wall sandwich panels have been widely used in many applications (e.g. transportation vehicles, modern buildings, and aerospace structures) due to their superior sound insulation properties over a wide frequency range and excellent mechanical properties. Poroelastic materials have been applied as the sandwich core within a double-wall (or multilayered) panel in order to improve the sound insulation performance. Based on Biot's theory [1], Bolton et al. [2] developed an analytical model for sound transmission through laterally infinite double-wall panels lined with poroelastic materials and have validated the model experimentally. Lee et al. [3] simplified the method of Bolton et al. by considering only the energetically dominant wave with negligible shear wave contributions and the poroelastic material was treated as a layer of equivalent fluid.

The modelling of sound transmission through realistic sandwich panels, however, needs to take into account the finite nature of the structure. Leppington et al. [4] employed a modal superposition theory to model the sound transmission through a pair of rectangular elastic plates with simply supported boundary condition. Using the same method, Xin et al. [5] studied theoretically the vibroacoustic response of a clamped double-panel partition enclosing an air cavity. Xin and Lu [6] then considered both fully clamped and simply supported boundary conditions through an analytical and experimental investigation. Daudin and Liu [7] extended these studies to consider clamp mounted double-wall panels lined with poroelastic materials.

In many practical applications (for example, aircraft and high-speed trains) for sound insulation purposes, the presence of an external flow is common and hence the effects on sound transmission

must be considered. Koval [8] has found that the external flow affect significantly the STL of an infinite single-wall panel. Zhou et al. [9] extended the work of Bolton et al. [2] to account for the external flow effect on the STL of double-wall panels with poroelastic linings. Liu and Sebastian [10] considered the effects of both an external and an internal mean flow on the sound transmission through double-wall sandwich panels. All these studies have shown that the presence of an external flow improves the sound insulation performance of the sandwich panels.

To the best knowledge of the authors, the problem of sound transmission through double-wall panels considering finite dimensions, poroelastic materials, and an external mean flow has yet to be addressed theoretically. In spirit of the previous works (e.g. [6, 7, 9]), the present study aims to develop a theoretical model for this problem, with a focus on the coupled effects of the external mean flow and the clamped boundary on the STL.

## 2. Theoretical formulation

### 2.1 Description of the system

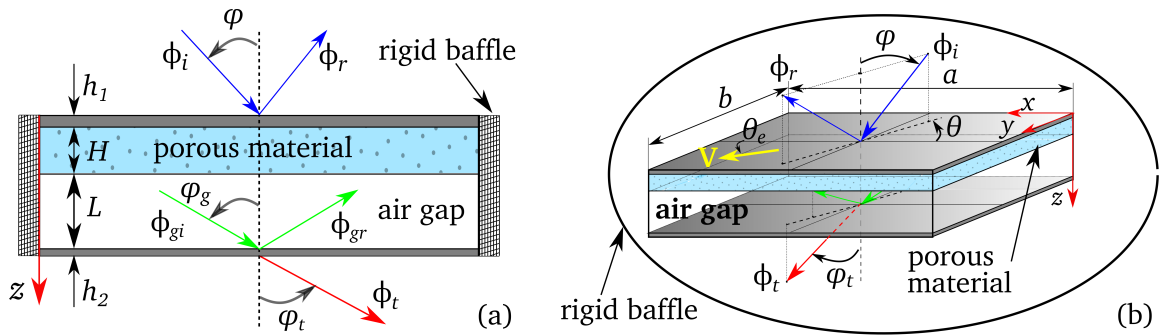


Figure 1: Schematic diagram of sound wave transmission through the double-wall panel of the BU configuration: (a) side view, (b) perspective view.

As illustrated in Fig. 1, the double-wall sandwich panel system consists of two parallel homogeneous thin elastic plates lined with a poroelastic layer. An air gap exists in between the poroelastic material and the facing plate. The system is situated in ambient air and a plane acoustic wave of unit amplitude is incident on the first (upper) plate and transmits through the system. The two rectangular plates are supposed to be fully clamped on each side to an infinite rigid baffle and the dimensions are  $a$  and  $b$  along the  $x$ - and  $y$ -axes. An external mean flow is considered in the incident field while the media in the air gap and the transmission side are stationary. The mean flow is assumed to be uniform in the external incident field and the boundary layer effect is ignored which is common in many simplified modelling of sound transmission problems [9, 10]. The direction of the incident wave can be described by two angles: i.e. the incidence angle  $\varphi$  between the incident wave and the normal of the  $x$ - $y$  plane, and the azimuthal angle  $\theta$  between the projection of the incident wave on the  $x$ - $y$  plane and the  $x$ -axis. The constant external flow is aligned along the  $x$ -axis ( $\theta_e = 0^\circ$ ).

The subsequent derivations are based on the BU (Bonded-Unbonded) configuration shown in Fig. 1 because this is a representative case for the general theoretical formulation, while other panel configurations (i.e. BB and UU [2]) are also considered in the present study. Readers may refer to a forthcoming article for the complete derivation in detail.

### 2.2 Wave propagation in porous materials

Biot's theory [1] is employed to describe wave propagation in poroelastic materials with details given in [2, 9, 11]. In this theory, porous materials are modelled as a solid and a fluid phase, and

two dilatational (frame and airborne) waves and one rotational (shear) wave are propagating in both phases. Lee et al. [3] compared the energy associated with the three wave types and concluded that the contribution of the rotational wave is always negligible compared to those of the frame and airborne waves. Moreover, the clamped boundary conditions restrict the mid-surface, in-plane motion of the panel and the shear wave propagation in the system. Therefore, there are only four wave components characterised by the amplitudes  $C_1$ – $C_4$  propagating within the porous material along the  $z$ -axis; the in-plane displacements of the plates and the porous layer and the shear stresses are also ignored. These wave amplitudes  $C_1$ – $C_4$  can be solved using the boundary conditions of a specific configuration (see Section 2.3.2), and then the expressions of normal displacement and stress components  $u_z$ ,  $U_z$  and  $\sigma_z$ ,  $s$  [2, 9, 11] can be determined through  $C_1$ – $C_4$ .

## 2.3 Vibroacoustic problem

### 2.3.1 Acoustic velocity potentials

On the incident side, the sound field can be decomposed as an incident wave and a reflected wave; thus the acoustic velocity potential can be expressed in a harmonic form:

$$\Phi_1 = \Phi_i + \Phi_r = e^{j\omega t - j(k_{ix}x + k_{iy}y + k_{iz}z)} + R e^{j\omega t - j(k_{ix}x + k_{iy}y - k_{iz}z)}, \quad (1)$$

where  $\Phi_i$  is the incident velocity potential with unit amplitude, and  $\Phi_r$  the velocity potential of the reflected wave with the amplitude  $R$ . The acoustic velocity potential in the external incident field satisfies the wave equation that considers a convective term [9, 10]:

$$D^2\Phi_1/Dt^2 = c^2\nabla^2\Phi_1, \quad (2)$$

in which the material derivate is  $D/Dt = \partial/\partial t + \mathbf{V} \cdot \nabla$ , and  $\mathbf{V}$  is the velocity vector of the external flow. Substituting the expression (1) of  $\Phi_1$  into Eq. (2) yields the wavenumber  $k_i$  as

$$k_i = k_i^s / (1 + M \sin \varphi \cos \theta), \quad (3)$$

where  $k_i^s = \omega/c$  is the wavenumber in the stationary medium and  $M = V/c$  is the Mach number of the external mean flow.

In the air gap field, the harmonic velocity potential can be expressed as

$$\Phi_g = \Phi_{gi} + \Phi_{gr} = I_g e^{j\omega t - j(k_{gx}x + k_{gy}y + k_{gz}z)} + R_g e^{j\omega t - j(k_{gx}x + k_{gy}y - k_{gz}z)}, \quad (4)$$

where  $I_g$  and  $R_g$  are the respective amplitudes of the incident and reflected waves in the air gap, and the wavenumber of the acoustic waves is  $k_g = k_i^s$ . The acoustic waves inside the air gap make an angle  $\varphi_g$  with the normal of the  $x$ - $y$  plane, as illustrated in Fig. 1(a). The azimuthal angle  $\theta$  remains unchanged across the panel system due to the Snell's law [9, 10, 12]. In the semi-infinite transmission field, only a single transmitted wave exists by assuming an anechoic termination with the harmonic expression of the velocity potential as

$$\Phi_t = T e^{j\omega t - j(k_{tx}x + k_{ty}y + k_{tz}z)}, \quad (5)$$

where  $T$  is the amplitude of the transmitted wave. Note that the air properties in both the air gap and the transmission field are identical; hence the wavenumber and the incidence angle remain the same in these two fields, i.e.  $k_t = k_g$ ,  $\varphi_t = \varphi_g$ .

In a stationary medium, the acoustic pressure and the normal acoustic particle velocity can be related to the corresponding velocity potential by

$$p = \rho_0 \partial \Phi / \partial t = j\omega \rho_0 \Phi, \quad v_z = -\partial \Phi / \partial z = jk_z \Phi; \quad (6)$$

whereas in the presence of an external mean flow, the acoustic pressure in the incident field is subject to the convective effect and hence  $p = \rho_0 D\Phi/Dt$ .

### 2.3.2 Boundary conditions

Since the bottom and upper plates are fully clamped to the rigid baffle, both the rotation moment and transverse displacement are equal to zero along the edges:

$$x = 0, a, \quad \forall \quad 0 < y < b, \quad w_1 = w_2 = 0, \quad \partial w_1 / \partial x = \partial w_2 / \partial x = 0, \quad (7a)$$

$$y = 0, b, \quad \forall \quad 0 < x < a, \quad w_1 = w_2 = 0, \quad \partial w_1 / \partial y = \partial w_2 / \partial y = 0; \quad (7b)$$

where  $w_1, w_2$  are the transverse displacements of the upper and bottom plates, respectively. Moreover, boundary conditions of continuous displacements, velocities and stresses must be satisfied at the plate-porous-air interfaces [2, 9, 10, 11]. First, three equations are satisfied on the first plate bonded to the porous layer:

$$(i) \quad v_{1z} = Dw_1/Dt, \quad (ii) \quad u_z = w_1, \quad (iii) \quad U_z = w_1. \quad (8)$$

At the interface of the porous layer and the air gap, three boundary conditions apply:

$$(i) \quad -\beta p_g = s, \quad (ii) \quad -(1 - \beta)p_g = \sigma_z, \quad (iii) \quad v_{gz} = (1 - \beta)\partial u_z / \partial t + \beta \partial U_z / \partial t; \quad (9)$$

and at the mid-surface of the bottom plate, two boundary conditions are satisfied:

$$(i) \quad v_{gz} = \partial w_2 / \partial t, \quad (ii) \quad v_{tz} = \partial w_2 / \partial t. \quad (10)$$

In the boundary conditions (8)–(10), the expressions of  $p_g, v_{1z}, v_{gz}, v_{tz}$  can be worked out from Eq. (6).

### 2.3.3 Modal decomposition

The transverse displacements  $w_1$  and  $w_2$  can be written as a modal decomposition [5, 6, 7]:

$$w_1(x, y, t) = \sum_{m,n} \phi_{mn}(x, y) \alpha_{1,mn} e^{j\omega t}, \quad w_2(x, y, t) = \sum_{m,n} \phi_{mn}(x, y) \alpha_{2,mn} e^{j\omega t}, \quad (11)$$

where  $\alpha_{1,mn}, \alpha_{2,mn}$  are the modal displacement coefficients of the upper and bottom plates. The modal function  $\phi_{mn}$  ensures that the clamped boundary conditions (7a) and (7b) are satisfied,

$$\phi_{mn}(x, y) = [1 - \cos(2m\pi x/a)] [1 - \cos(2n\pi y/b)]. \quad (12)$$

Substituting the expressions of  $\Phi_1, \Phi_g, \Phi_t, w_1, w_2$  and  $u_z, U_z, \sigma_z, s$  [2, 9, 11] into the boundary conditions (8)–(10), one obtains a matrix equation that can be resolved to determine the 8 unknowns  $R, I_g, R_g, T$  and  $C_1 - C_4$  in terms of  $\alpha_{i,mn}$  ( $i = 1, 2$ ).

### 2.3.4 The Galerkin method

It remains to solve the modal coefficients  $\alpha_{1,mn}$  and  $\alpha_{2,mn}$  for the closure of the entire problem. The Galerkin (weighted residual) method is used that sets the integral of a weighted residual of the modal function to zero and yields an arbitrarily accurate double-series solution [6]. The integral equations are obtained by applying the governing equations of plate flexural motions, i.e.

$$\int_0^b \int_0^a (D_1 \nabla^4 w_1 + m_1 \partial^2 w_1 / \partial t^2 - \rho_0 D\Phi_1 / Dt - \sigma_z - s) \cdot \phi_{mn}(x, y) \, dx \, dy = 0, \quad (13a)$$

$$\int_0^b \int_0^a (D_2 \nabla^4 w_2 + m_2 \partial^2 w_2 / \partial t^2 - \rho_0 \partial \Phi_g / \partial t + \rho_0 \partial \Phi_t / \partial t) \cdot \phi_{mn}(x, y) \, dx \, dy = 0. \quad (13b)$$

Substituting the expressions of  $\Phi_1, \Phi_g, \Phi_t, w_1, w_2$  and  $\sigma_z, s$  into Eqs. (13a) and (13b) leads to a set of infinite algebraic equations for the unknown modal coefficients  $\alpha_{1,mn}$  and  $\alpha_{2,mn}$ . To solve these equations numerically, a truncation of  $1 \leq m, n \leq N$  is needed resulting in a matrix of  $2N^2$  equations. Once the modal coefficients  $\alpha_{1,mn}, \alpha_{2,mn}$  are solved, the transmission coefficient  $\tau$ , i.e. the ratio of the transmitted and incident sound power, is simply obtained as  $|T|^2$  due to the unit incident wave amplitude. Finally, the sound transmission loss (STL) can be calculated via

$$\text{STL} = 10 \log_{10}(1/\tau) \quad (14)$$

### 3. Numerical results and discussion

Property parameters of the plates, porous layer and ambient air used in previous works [2, 9, 10] are taken in this study. The two plates have identical properties for the three configurations with the thicknesses of  $h_1 = 1.27$  mm and  $h_2 = 0.762$  mm for the first and second plates. The thickness of the polyurethane foam is  $H = 41$  mm for the BB configuration and  $H = 27$  mm for BU and UU; the depth of the air gap(s) varies from  $L = 14$  mm for BU to  $L_1 = L_2 = 7$  mm for UU, resulting in the same total thickness  $H_t = 41$  mm. The sufficient mode number  $N$  is dependent on frequencies and panel dimensions [7], and a convergence check has been carried out to determine the  $N$  value.

#### 3.1 Model validation

Two test cases are considered in order to validate the theoretical model and numerical code used in this study, i.e. the sound transmission across infinite sandwich panels without and with an external mean flow by Bolton et al. [2] and Zhou et al. [9], respectively. The original data were for random transmission loss in a diffuse field, and the results of a single incident wave are calculated using their theories for the comparisons in Figs. 2(a) and 2(b). A relatively large panel of  $a = b = 1.0$  m is used to approximate the infinite panels considered in [2, 9].

As shown in Fig. 2(a), the agreement between the current model and Bolton et al.'s theory is satisfactory for all configurations, especially at low frequencies below 100 Hz. The current model for finite panels slightly underestimates the STL levels predicted by the theory for infinite panels [2]. Moreover, in the mid-high frequency range, dense peaks and dips over the STL spectra of the current model are associated with the inherent modal behaviour of the finite panel system and is dominated by the bottom plate on the transmission side [6]. The relatively large dips at about 250 Hz for the BU and UU configurations and at about 1100 Hz for the BB configuration, however, are due to the mass-air-mass resonance which are insensitive to the lateral dimension of the panel [6, 10].

For brevity, the second case shown in Figs. 2(b) is for the UU configuration only. It can be seen that above the mass-air-mass resonance frequency the agreement between the two models is similar to that in Figs. 2(a). The striking feature of the finite panel, however, is the remarkably high STL below the mass-air-mass resonance frequency. This phenomenon is inherently due to the clamped boundary imposed on the finite panel as has been observed previously (e.g. [5, 6, 7]), and the presence of the external mean flow magnifies this effect and shifts up the critical frequency where this effect occurs, which will be discussed further in Section 3.3. The two test cases have reasonably validated the theoretical model developed in this study.

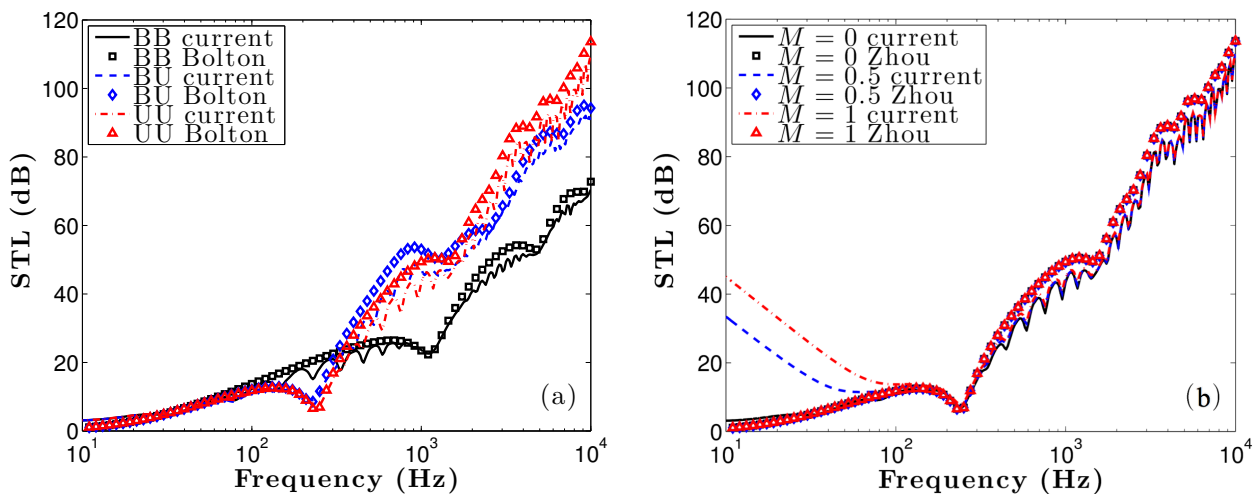


Figure 2: Comparison of STL spectra between the present study and previous works: (a) without external flow [2], (b) with external flow [9],  $a = b = 1.0$  m,  $\varphi = 0^\circ$ ,  $\theta = 45^\circ$ .

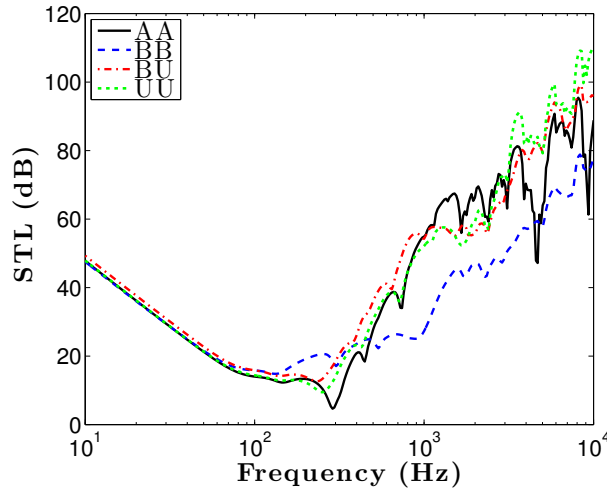


Figure 3: Comparison of STL spectra among the four panel configurations,  $a = b = 0.5$  m,  $M = 0.5$ ,  $\varphi = 30^\circ$ ,  $\theta = 45^\circ$ .

### 3.2 Effects of panel configurations

Apart from the BB, BU and UU configurations, another configuration with only an air gap in between the two facing plates (referred to as AA) is considered to assess the effects of poroelastic materials. The STL results of all four configurations are shown in Fig. 3. In the low-frequency range, the STL levels of all configurations appear very close because the clamped boundary imposes a rigorous constraint on panel vibration and governs the STL characteristics at low frequencies. In the mid-high frequency range above 500 Hz, the BB configuration exhibits the lowest STL levels due to the lack of an air gap. Comparing the AA configuration with the others, it can be seen that the dips in the STL spectra are attenuated by the damping effect of the porous material, in particular the strong dips due to the standing wave resonance [5, 6, 11] at about 4500 Hz and 9000 Hz. Moreover, the UU configuration exhibits the best overall sound insulation properties among the four configurations. The excellent high-frequency performance can be attributed to the extra wave reflection induced by the two air gaps and hence enhanced sound absorption within the poroelastic layer.

### 3.3 Effects of finite dimensions

Figs. 4(a) and 4(b) compare the STL spectra among three finite panels with different lateral extensions as well as an infinite panel with and without the external mean flow, respectively. Consider first the case of no external flow in Fig. 4(a). The STL spectrum of the large panel of  $a = b = 1.0$  m can be well approximated by that of the infinite panel over almost the entire frequency range. Apart from the dense dips at high frequencies as a result of complex modal behaviours, the finite extension of the panel comes into effect distinctly only at sufficiently low frequencies below the fundamental natural frequency  $f(1, 1)$  where the wave length of the sound wave becomes relatively long compared with the size of the panel [7]. For the same reason, as the panel dimension decreases gradually this effect of finite dimensions becomes more obvious in terms of the significantly enhanced STL levels and the enlarged frequency range of this effect.

Xin and Lu [6] compared the clamped and simply supported boundary conditions and have shown that the increased constraint on panel vibration of the clamped condition raises the panel stiffness and hence increases significantly the  $(1, 1)$  modal frequency and the STL levels below this frequency. The reduction of the panel dimensions, therefore, behaves similarly to the increased constraint by increasing the panel stiffness and hence the STL below  $f(1, 1)$ . Beyond the  $(1, 1)$  modal frequency, however, the STL spectra of the finite panels exhibit similar trends as the infinite counterpart which can be regarded as an asymptotic form of the finite panels.



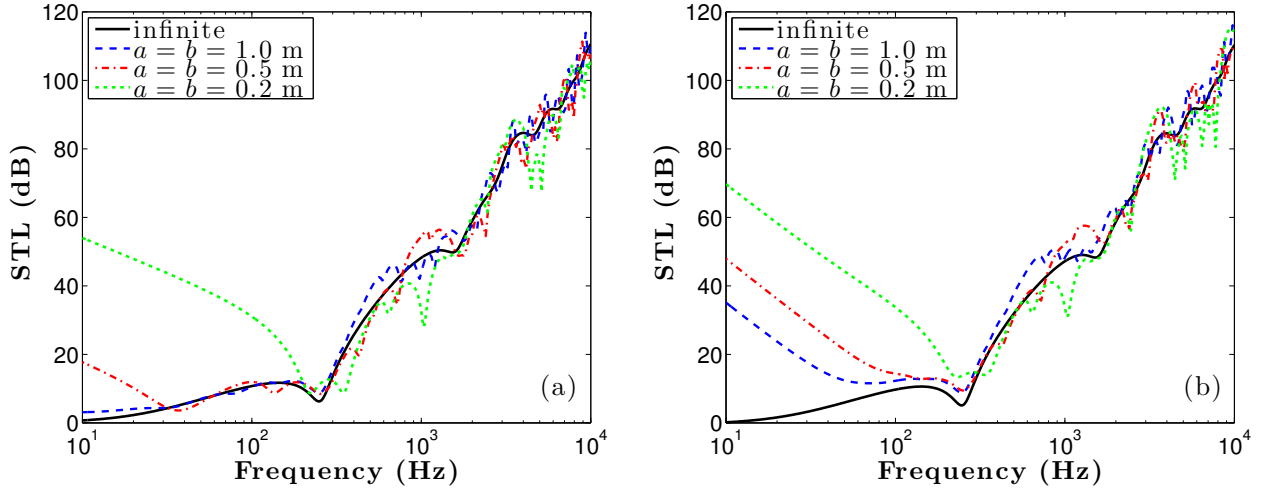


Figure 4: Effects of finite dimensions on the STL spectra for the UU configuration,  $\varphi = 30^\circ$ ,  $\theta = 45^\circ$ , (a)  $M = 0$ , (b)  $M = 0.5$ .

### 3.4 Effects of external flow Mach numbers

Fig. 4(b) shows this comparison in the presence of an external mean flow  $M = 0.5$ . It has been known that a convective mean flow can enhance the transmission loss across an elastic panel due to the aerodynamic (or acoustic radiation) damping effect (e.g. [10, 13]). The effect of the external mean flow is evident in Fig. 4(b) through the further increased panel stiffness which elevates significantly the STL levels of the three finite panels below the  $(1, 1)$  modal frequency. Comparing the STL spectra in Figs. 4(a) and 4(b), it is shown that the convective flow effect of added stiffness is huge for the large square panel of 1.0 m width with a STL gain about 35 dB at 10 Hz, for example. However, this effect becomes progressively less distinct as the panel dimensions decrease.

The effect of the external flow Mach number on the transmission loss can be seen more obviously in Fig. 5 for a series of Mach numbers. As  $M$  increases, three phenomena can be observed: (1) the fundamental natural frequency  $f(1, 1)$  is shifted up to higher frequencies until it reaches about 250 Hz for  $M = 1$ ; (2) the noticeable resonances at low frequencies below 250 Hz in the case of  $M = 0$  are attenuated gradually due to the aerodynamic damping effect exerted by the external flow; and most importantly, (3) the STL levels are enhanced significantly below the  $(1, 1)$  modal frequency.

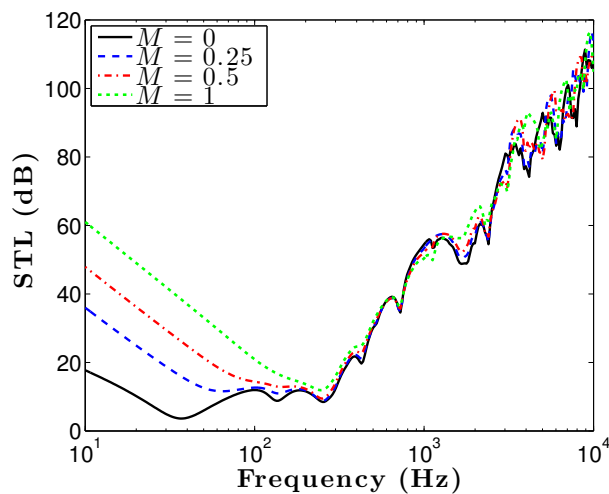


Figure 5: Effects of external flow Mach numbers on the STL spectra for the UU configuration,  $a = b = 0.5$  m,  $\varphi = 30^\circ$ ,  $\theta = 45^\circ$ .

## 4. Conclusions

In this paper, a theoretical model has been developed to study the effects of an external mean flow on the sound transmission across finite clamped double-wall sandwich panels lined with poroelastic materials. Biot's [1] theory was used to describe the wave propagation in the poroelastic material, and a modal decomposition and the Galerkin method [6, 7] were employed to account for the clamped boundary of finite panels. Details of the derivation will be presented in a forthcoming article. The theoretical model has been validated against previous results [2, 9] with and without an external mean flow. It can be concluded that the UU case exhibits the optimal overall sound insulation performance. The effects of the external mean flow on the STL are significant in the low-frequency range and are coupled with the effects of the finite dimensions and clamped boundary. The added panel stiffness by the aerodynamic damping of the external flow shifts up the fundamental natural frequency of the finite panel system and raises the STL levels significantly below this modal frequency along with the attenuation of low-frequency resonances.

## REFERENCES

1. Biot, M. A. Theory of propagation of elastic waves in a fluid-saturated porous solid I. Low-frequency range. II. Higher frequency range, *Journal of the Acoustical Society of America*, **28** (2), 168–191, (1956).
2. Bolton, J. S., Shiau, N. M. and Kang, Y. J. Sound transmission through multi-panel structures lined with elastic porous materials, *Journal of Sound and Vibration*, **191** (3), 317–347, (1996).
3. Lee, J. H., Kim, J. and Kim, H. J. Simplified method to solve sound transmission through structures lined with elastic porous material, *Journal of the Acoustical Society of America*, **110** (5), 2282–2294, (2001).
4. Leppington, F. G., Broadbent, E. G. and Butler, G. F. Transmission of sound through a pair of rectangular elastic plates, *IMA Journal of Applied Mathematics*, **71** (6), 940–955, (2006).
5. Xin, F. X., Lu, T. J. and Chen, C. Q. Vibroacoustic behavior of clamp mounted double-panel partition with enclosure air cavity, *Journal of the Acoustical Society of America*, **124** (6), 3604–3612, (2008).
6. Xin, F. X. and Lu, T. J. Analytical and experimental investigation on transmission loss of clamped double panels: Implication of boundary effects, *Journal of the Acoustical Society of America*, **125** (3), 1506–1517, (2009).
7. Liu, Y. and Daudin, C. Analytical modelling of sound transmission through finite clamped double-wall panels lined with poroelastic materials, *Composite Structures*, **172**, in press, (2017).
8. Koval, L. R. Effect of air flow, panel curvature, and internal pressurization on field-incidence transmission loss, *Journal of the Acoustical Society of America*, **59** (6), 1379–1385, (1976).
9. Zhou, J., Bhaskar, A. and Zhang, X. Sound transmission through a double-panel construction lined with poroelastic material in the presence of mean flow, *Journal of Sound and Vibration*, **332** (16), 3724–3734, (2013).
10. Liu, Y. and Sebastian, A. Effects of external and gap mean flows on sound transmission through a double-wall sandwich panel, *Journal of Sound and Vibration*, **344**, 399–415, (2015).
11. Liu, Y. Sound transmission through triple-panel structures lined with poroelastic materials, *Journal of Sound and Vibration*, **339**, 376–395, (2015).
12. Liu, Y. and He, C. Diffuse field sound transmission through sandwich composite cylindrical shells with poroelastic core and external mean flow, *Composite Structures*, **135**, 383–396, (2016).
13. Liu, Y. and He, C. Analytical modelling of acoustic transmission across double-wall sandwich shells: Effect of an air gap flow, *Composite Structures*, **136**, 149–161, (2016).